Journal of Geriatric Cardiology (2019) 16: 764–774

Research Article · Open Access ·

Qishen capsule safely boosts cardiac function and angiogenesis via the MEK/ERK pathway in a rat myocardial infarction model

Cai-Xia GUO[1], Zhi-Yuan LI[1,#], Jin-Bang NIU[2], Shuan-Cheng FAN[2], Si-Yu YAN[1], Pei-Pei LU[1], Yan-Ni SU[1], Li-Hong MA[1,#]

[1]*State Key Laboratory of Cardiovascular Disease, Fuwai Hospital, National Center for Cardiovascular Diseases, Chinese Academy of Medical Sciences and Peking Union Medical College, Beijing, China*

[2]*Shanghai Kai Bao Pharmaceutical Co., Ltd, Shanghai, China*

Abstract

Background Qishen (QS) capsules, a Traditional Chinese Medicine, has been widely used to treat coronary heart disease in China. However, evidence of its effectiveness remains unclear. **Methods** To explore whether QS has cardioprotective efficacy and/or promotes angiogenesis after myocardial infarction (MI), we performed experiments in a preclinical rat MI model. One month after left anterior descending coronary artery ligation, the rats received either QS solution (0.4 g/kg/day) or the same volume of saline by intragastric injection for four weeks. **Results** Echocardiographic and hemodynamic analyses demonstrated relatively preserved cardiac function in MI rats administered QS. Indeed, QS treatment was associated with reduced infarct scar size and heart weight index, and these beneficial effects were responsible for enhancing angiogenesis. Mechanistically, QS treatment increased phosphorylation of protein kinase B (Akt) and downregulated phosphorylation of mitogen-activated protein kinase/extracellular-regulated kinase (MEK/ERK). **Conclusions** QS therapy can improve the cardiac function of rats after MI by an underlying mechanism involving increased angiogenesis, at least partially via activation of the Akt signaling pathway and inhibition of MEK/ERK phosphorylation.

J Geriatr Cardiol 2019; 16: 764–774. doi:10.11909/j.issn.1671-5411.2019.10.008

Keywords: Angiogenesis; Cardioprotective efficacy; Qishen capsule

1 Introduction

Myocardial infarction (MI) is a major public health problem that results from irreversible reduction of cardiomyocytes, scar formation, and ventricular remodeling. Moreover, cardiac dysfunction is partially associated with significant reduction in capillary density, which can lead to massive cardiomyocyte apoptosis.[1–3] Inducing neovascularization and decreasing myocyte apoptosis in infarct border regions are currently considered reliable approaches to modify the pathological changes of ventricular remodeling during the chronic phase of MI.[4] Therefore, a large number of diverse strategies to boost angiogenesis are being explored in the pre-clinical setting.[5,6]

Traditional Chinese Medicine (TCM) explains primary cause of MI during the chronic phase as Qi inadequacy and blood stasis. Some herbs have demonstrated efficacy and safety for the treatment of cardiovascular diseases in both humans and animal models.[7–9] One such TCM prescription is Qishen (QS) capsules, an extract obtained from 15 types of herbs including Astragalus membranaceus, Salvia miltiorrhiza, Panax ginseng, Wolfiporia extensa, Panax notoginseng, Hirudo, safflower, Ligusticum wallichii, hawthorn, cattail pollen, Radix Polygoni Multiflori Praeparata, Radix Puerariae, Scutellaria baicalensis, Scrophularia ningpoensis, and licorice.

Since being approved for the treatment of coronary heart disease by China Food and Drug Administration in 2008, QS has become broadly used in China for the treatment of coronary heart disease and unstable angina pectoris. Although QS administration exhibited cardioprotective functions in clinical trials,[10,11] the exact mechanism by which QS exerts beneficial effects remains unclear. As such, this study appraises the effects of QS in rats after MI.

[#]**Correspondence to:** Zhi-Yuan LI & Li-Hong MA, State Key Laboratory of Cardiovascular Disease, Fuwai Hospital, National Center for Cardiovascular Diseases, Chinese Academy of Medical Sciences and Peking Union Medical College, Beijing, China. E-mails: yuanfang6707@sina.com (LI ZY) & mlh8168@163.com (MA LH)

Received: August 10, 2019 **Revised:** September 20, 2019
Accepted: October 17, 2019 **Published online:** October 28, 2019

2 Methods

2.1 Animals

Adult male Sprague-Dawley rats (weighing: 200–220 g) were obtained from Vital River Laboratory Animal Inc. (Beijing, China). All experimental procedures complied with the Guide for the Care and Use of Laboratory Animals published by the National Institutes of Health (Bethesda, MD), and were approved by the Care of Experimental Animals Committee of Fuwai Hospital, Beijing, China (2013-5-100-HX). Rats were housed with a 12-h light/dark cycle under uniform conditions of humidity and temperature.

2.2 Preparation of QS solution

QS ultrafine powder (Henan XinYi Pharmaceutical, Henan, China) in this study was dissolved in physiological saline at a concentration of 100 mg/mL. Fresh suspensions of QS ultrafine powder were prepared in darkness each day. To achieve quality control of QS capsules, herbal drugs were standardized and verified against marker compounds according to the Chinese Pharmacopoeia (2005).

2.3 Animal surgery and experimental grouping

MI was induced in rats by permanent ligation of the left anterior descending coronary artery (LAD) at the same level. All procedures were performed as previously described.[12–14] Briefly, rats were intraperitoneally anesthetized with 10% chloralhydrate (3 mL/kg) and artificially ventilated after oral intubation using a volume-cycled small-animal ventilator (Harvard Apparatus, Holliston, MA). The hearts were then rapidly exteriorized through left anterolateral thoracotomy, and the LADs were ligated with the 6–0 silk suture around a 2–3 mm distance between the junction of the pulmonary trunk and left appendage. The sham-operation group underwent uniform surgical procedures without coronary ligation. Successful ligation of the LAD was confirmed by abnormal movement of the anterior wall and observation of myocardial blanching.[15]

Four weeks after MI, surviving rats with left ventricular ejection fraction less than 60% (as measured by ultrasonic assessments) were randomized into four groups: sham (n = 8), sham with QS treatment (Sham + QS, n = 8), MI control (MI, n = 14), and QS capsule treatment (MI + QS, n = 14). The MI + QS and the Sham + QS groups were treated with 0.4 g/kg/day QS by intragastric injection for four weeks. Sham and MI groups were perfused with the same volume of saline.

2.4 Transthoracic echocardiography and intraoperative hemodynamics

Transthoracic echocardiography was performed at four weeks (baseline) and eight weeks (endpoint) after MI using a 12-MHz phased-array transducer (Sonos 7500, Phillips, Andover, MA). After two-dimensional graphics were obtained, measurements were performed in a long-axis view at the papillary muscle level. Left ventricular end-systolic diameter (LVESd) and end-diastolic diameter (LVEDd) were detected. In addition, left ventricular fractional shortening (LVFS) and left ventricular ejection fraction (LVEF) were calculated as follows: LVFS (%) = [(LVEDd − LVESd)/LVEDd] × 100, and LVEF (%) = [($LVEDd^3$ − $LVESd^3$)/$LVEDd^3$] × 100. Parameters were performed over three consecutive heart cycles and the average was used for analysis. Measurements were analyzed by a specialized sonographer blinded to the treatment. Left heart catheterization was carried out eight weeks after MI to evaluate cardiac function. Prior to catheterization, the rats were anesthetized by intraperitoneal injection of 10% chloralhydrate (3 mL/kg). Subsequently, the rats were mechanically ventilated and the anterior chest walls were opened. The left ventricular (LV) pressure curve, maximal rate of LV pressure rise and fall (± dp/dt_{max}), and LV end-diastolic pressure (LVEDP) were recorded, while the catheter was direct inserted into LV.

2.5 Histological analysis

At the end of the experiment, animals were euthanized and heart tissues were harvested and weighed. Heart weight index value for each animal was expressed as the ratio of heart weight to body weight. Next, hearts were fixed in 10% formalin for 24 h for the preparation of paraffin sections, which were stained with hematoxylin and eosin, Masson's trichrome, and picrosirius red for histological analysis including assessment of inflammation.

Infarct scar size and area were measured as recently described for Masson's trichrome staining, with the blue area regarded as scar tissue and taken as the infarct scar area.[15] Five sections per heart (five hearts per experimental group) were scanned and computerized using Image-Pro Plus software (Media Cybernetics, Rockville, MD). Infarct scar area was calculated as the ratio of infarct scar area to the total LV area. Infarct scar size was expressed as the sum of epicardial and endocardial scar lengths divided by the sum of LV epicardial and endocardial circumferences. The thinning ratio was also quantified, which is defined as the ratio of infarct wall thickness to contralateral non-infarcted wall thickness.

Picrosirius red-stained 6-mm sections of paraffin-embedded tissue were analyzed for collagen content evaluation within the infarct zone.[12,13] Collagen type III was stained green, while collagen type I was stained as red or yellow fibers. Six sections of each heart (three hearts per group)

were evaluated with a 400 × objective lens under a polarized light microscope.

2.6 Ultrastructure analysis with transmission electron microscopy (TEM)

At the end of experiments, rat hearts were removed. Three samples of fresh myocardial tissue (approximately 1 mm in size) were obtained 3 mm from the peri-infarct area of the LV.[14] Tissues were fixed with 5% glutaraldehyde overnight at 4°C, washed three times with phosphate-buffered saline, and fixed again with 1% osmium tetraoxide for 2 h. Ultra-thin sections were acquired by standard procedures. A JEOL 1400-EX TEM (Tokyo, Japan) was utilized to review three randomly chosen fields per rat (three rats per group), for which three 8000 × images of peri-infarct area and three 12000 × images of capillaries were acquired.

2.7 Immunohistochemistry and immunofluorescence

Immunohistochemical and immunofluorescence staining on 4-mm tissue sections were performed as previously described.[16,17] To assist with capsule vessel identification, prepared transverse paraffin sections were stained with antibodies against CD31 (1:300, mouse monoclonal; Abcam, Cambridge, UK). Arteriolar densities were evaluated by immunofluorescence staining of sections with an anti-alpha smooth muscle actin antibody (α-SMA, 1:500, mouse monoclonal; Abcam). Angiogenesis in infarct and peri-infarct regions was evaluated by capillary and arteriolar densities, respectively. Numbers of capillaries and arteries were counted in 10 fields per section in both the infarct and peri-infarct border zones of hearts from six rats per group at 200 × magnification. Densities are expressed as counts of capillaries or arterioles per field by a trained observer blinded to the identity of each animal. To investigate the survival of cardiomyocytes in the peri-infarct region, sections were assessed by staining with antibodies against sarcomeric alpha actinin (α-actinin, 1:100, mouse monoclonal; Abcam) and desmin (1:1000, rabbit polyclonal; Abcam). Subsequently, sections were stained with antibodies against vascular endothelial growth factor (VEGF; 1:50, goat polyclonal; R&D Systems, Minneapolis, MN) and α-SMA (1:500, mouse monoclonal; Abcam) to assess the levels of angiogenesis. Fluorescence was observed under a Leica SP8 confocal laser-scanning microscope (Wetzlar, Germany).

2.8 Western blot

Proteins were prepared from peri-infarct myocardial tissues. Equal amounts of protein (60 μg/lane) were separated by electrophoresis for western blotting analysis. Subsequently, proteins were transferred to a polyvinylidene fluoride membrane (Millipore, Billerica, MA) using a semi-dry electroblotting apparatus (Bio-Rad, Hercules, CA). Next, membranes were blocked for 2 h at room temperature in 5% skim milk and incubated overnight at 4°C with primary antibodies against phosphorylated and total mitogen-activated protein kinase (MEK), and phosphorylated and total extracellular regulated protein kinase (ERK1/2) from Cell Signaling Technology (Danvers, MA). After washing, membranes were incubated for 2 h at room temperature in blocking solution containing horseradish peroxidase-conjugated secondary antibodies at 1:10000. Subsequently, membranes were washed and processed for analysis using a Chemiluminescence Detection Kit (Pierce, Rockford, IL) according to the manufacturer's instructions. An anti-rabbit-GADPH antibody (1:1000) was used as a housekeeping control. Target signals were semi-quantitatively analyzed with a Quantity One system (Bio-Rad).

2.9 Enzyme-linked immunosorbent assay (ELISA)

ELISA for VEGF was performed with a commercially available ELISA kit (Quantikine® Rat VEGF, R&D Systems) as previously described.[18]

2.10 Quantitative real-time polymerase chain reaction (qPCR)

qPCR was used to identify expression levels of angiogenesis-related genes as previously described. Briefly, tissue samples were harvested, flash frozen in liquid nitrogen, and stored at –80 °C until processing. Messenger ribonucleic acid (mRNA) was isolated using a Superscript II RT Kit (Applied Biosystems, Foster City, CA), deoxyribonuclease was used to ensure no plasmid DNA contaminates the final product. Each primer was selected from a region that was not conserved among different species, in order to ensure specificity and avoid amplification of endogenous rat vascular endothelial growth factor-α (VEGF-α) and hypoxia inducible factor-1α (HIF-1α). Sequences of primers for VEGF were 5'-CAATGATGAAGCCCTGGAGT-3' (sense) and 5'-TCTTTCTTTGGTCTGCATTCAC-3' (antisense); and for HIF-1α were 5'-TCATCCAAGGAGCCTTAACC-3' (sense) and 5'-CGCTTCCTCTGAGCATTCTG-3' (antisense). The sizes of PCR products for VEGF-α and HIF-1α were 144 and 108 bp, respectively. Amplification, fluorescence detection and post-processing calculations were performed using a Lightcycler apparatus (Roche, Basel, Switzerland).

2.11 Statistical analyses

Data were analyzed with SPSS 16.0 (IBM, Armonk, NY). All data were expressed as mean ± SD. Differences among

groups were tested with one-way analyses of variance (ANOVA) followed by post hoc Least Significant Difference (LSD) test. Comparisons between two groups were performed with Student's *t*-test. Two-sided *P*-values were used, and a $P < 0.05$ was considered statistical significant.

3 Results

3.1 Basic parameters

Out of the 70 rats, ten died during the MI procedure and seven died during the first week after MI. These deceased animals were excluded from statistical analyses. Another nine rats were excluded from the experiment because the baseline echocardiographic data (four weeks after MI) did not satisfy the standard for successful induction of MI (LVEF < 60% and motion abnormalities of the left ventricular wall). Rats were randomly selected from each group to perform echocardiography, of which one rat in the MI + QS group died before echocardiographic examination; this was regarded to be the result of anesthetic complications. Subsequently, one rat from both MI and QS groups died during the treatment process (5–8 weeks) (Table 1).

3.2 QS preserved left ventricular function in MI rats

As shown in Figure 1A, echocardiography images were obtained at four weeks (baseline) and eight weeks (endpoint) after MI. Baseline echocardiography displayed no statistical significance between the MI group and the MI + QS group (Table 1). At the endpoint, significant improvements in systolic function index, percent ejection fraction, and fractional shortening were observed in the MI + QS group compared with the MI group ($P < 0.05$, Table 1, Figure 1B & 1C). In parallel, LVEDd and LVESd were both lower in the MI + QS group ($P < 0.05$, Table 1).

Hemodynamic analysis verified the efficacy of QS treatment on cardiac function. Indeed, improvements in both LVEDP and maximum -dp/dt occurred in the QS-treated group compared with the MI group, with an observed decrease in LVEDP and increase in dp/dt after QS treatment ($P < 0.05$, Figure 1D & 1E). The MI + QS group also exhibited a lower maximum -dp/dt than the control group albeit not statistical significant.

3.3 QS treatment enhanced beneficial effects on cardiovascular morphogenesis

3.3.1 Limits infarct scar size

At the endpoint, heart weigh index significantly decreased in the MI + QS group compared with the MI group ($P < 0.05$, Figure 2A). In addition, we found that QS remarkably reduced both infarct scar size and infarct scar area, and the thinning ratio maintained a higher value ($P < 0.05$, Figure 2B-D). These results reflected relative preservation of cardiac architecture in the MI + QS group compared with the MI group. Macroscopically, the hearts of MI rats were more spherical to those of untreated MI rats, indicating attenuation of LV global remodeling after QS treatment. In addition, hematoxylin and eosin staining demonstrated that severe inflammatory cell infiltration occurred in all infarct hearts, but was reduced in the MI + QS group compared with the MI control group. Notably, in the MI + QS group, healthy muscle tissue was observed in the infarct regions, which was absent in the MI group (Figure 3A).

3.3.2 Collagen content in the infarct region

Given the reductions of infarct scar size with cardiospheres, we looked for a potential anti-fibrotic effect. Masson's trichrome staining revealed no collagen deposition in sham or Sham + QS groups. In MI control animals, collagen deposition was clearly detected and little healthy muscle tissue was observed. In contrast, a reduction in fibrous tissue

Table 1. Echocardiography measurements in different groups.

Group	Time point	*n*	LVEF	LVFS	LVEDd	LVESd
Sham	Baseline	8	76.88 ± 6.94	41.29 ± 6.94	0.74 ± 0.09	0.44 ± 0.09
	Endpoint	8	77.21 ± 8.21	41.95 ± 9.02	0.71 ± 0.08	0.42 ± 0.10
Sham + QS	Baseline	8	77.86 ± 5.69	40.89 ± 6.54	0.78 ± 0.12	0.45 ± 0.13
	Endpoint	8	78.65 ± 6.78	41.20 ± 8.05	0.75 ± 0.08	0.43 ± 0.06
MI	Baseline	14	50.99 ± 4.90	23.01 ± 2.78	0.96 ± 0.05	0.74 ± 0.05
	Endpoint	12	44.93 ± 5.66*	19.79 ± 3.02*	1.01 ± 0.09*	0.81 ± 0.08*
MI + QS	Baseline	14	49.22 ± 6.63	22.03 ± 3.67	0.89 ± 0.09	0.69 ± 0.09
	Endpoint	13	57.21 ± 8.4$^{*\Delta}$	26.89 ± 5.64$^{*,\Delta}$	0.91 ± 0.08$^{\Delta}$	0.67 ± 0.09$^{\Delta}$

Data are presented as means ± SD. $^{*}P < 0.05$ *vs.* baseline, $^{\Delta}P < 0.05$ *vs.* MI group at endpoint. LVEDd: left ventricular end-diastolic diameter; LVEF: left ventricular ejection fraction; LVESd: left ventricular end-systolic diameter; LVFS: left ventricular fractional shortening; MI: myocardial infarction; QS: Qishen capsule.

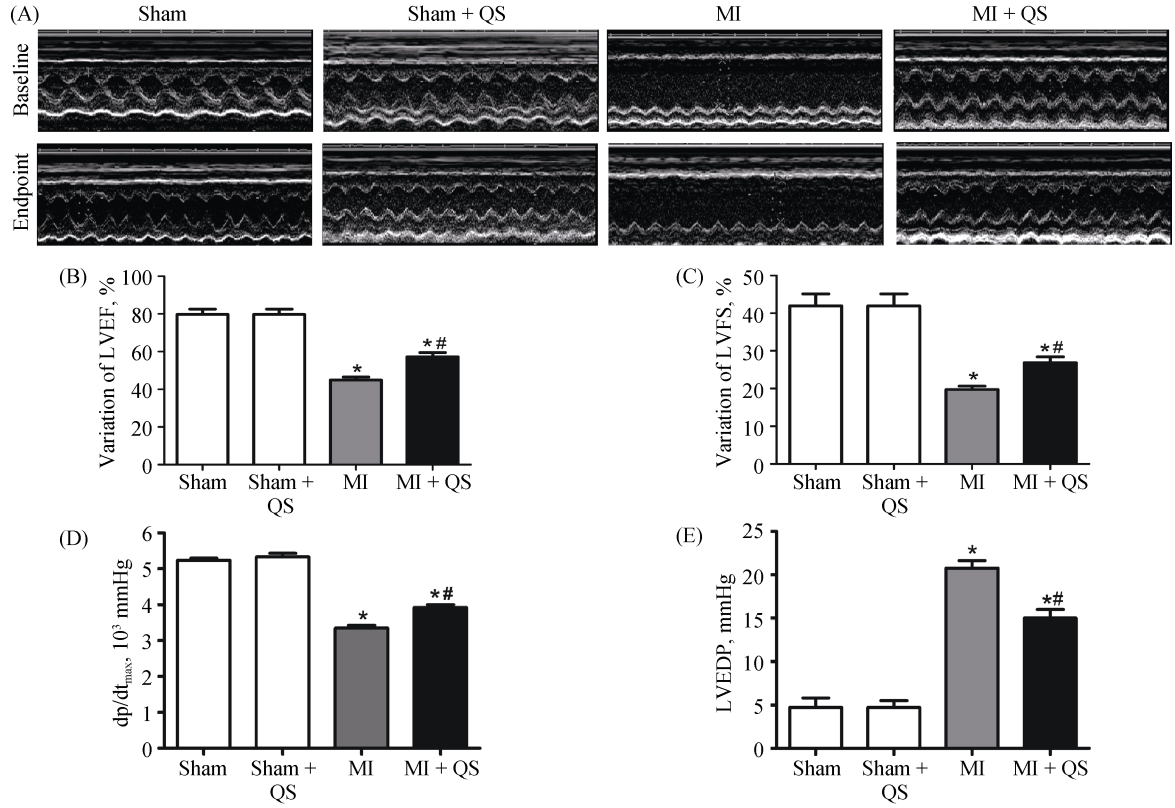

Figure 1. Echocardiography and hemodynamics assessment of cardiac function. (A): Representative images of echocardiography at the baseline and the endpoint; (B): echocardiography measurement of LVEF; (C): echocardiography measurement of LVFS at the endpoint; (D): hemodynamics assessment of dp/dt_{max}; and (E): hemodynamics assessment of LVEDP at the endpoint (n = 5 in each group). The baseline is four weeks after infarction, and the endpoint is eight weeks after infarction. $^{*}P < 0.05$ compared with the Sham group, $^{\#}P < 0.05$ compared with the MI group. dp/dt_{max}: left ventricular pressure maximal rate of rise; LVEDP: left ventricular end-diastolic pressure; LVEF: left ventricular ejection fraction; LVFS: left ventricular fractional shortening; MI: myocardial infarction; QS: Qishen capsule.

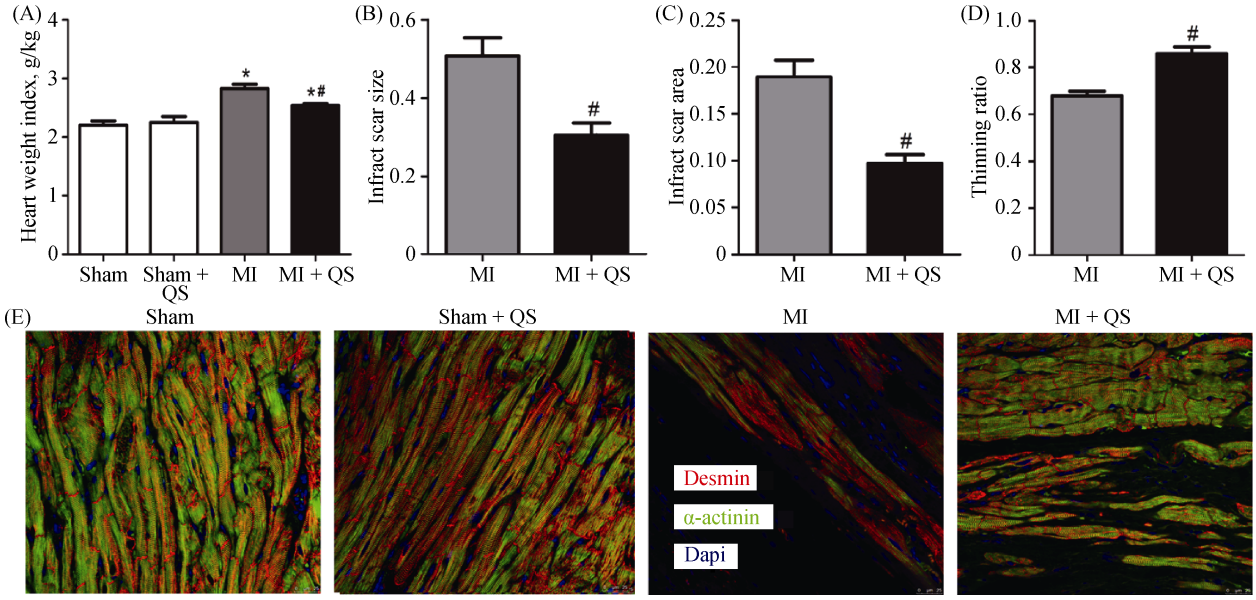

Figure 2. Quantitative histological analysis and viable myocardium identification. (A): Representative heart weight index; (B): quantitative analysis of infarct scar size; (C): quantitative analysis of infarct scar area; (D): quantitative analysis of thinning ratio with Masson's trichrome staining; and (E): representative immunofluorescence of viable myocardium positive for desmin and α-actinin in the infarct area. n = 6 in each group. The magnification is 400 ×. $^{*}P < 0.05$ compared with the Sham group, $^{\#}P < 0.05$ compared with the MI group. MI: myocardial infarction; QS: Qishen capsule.

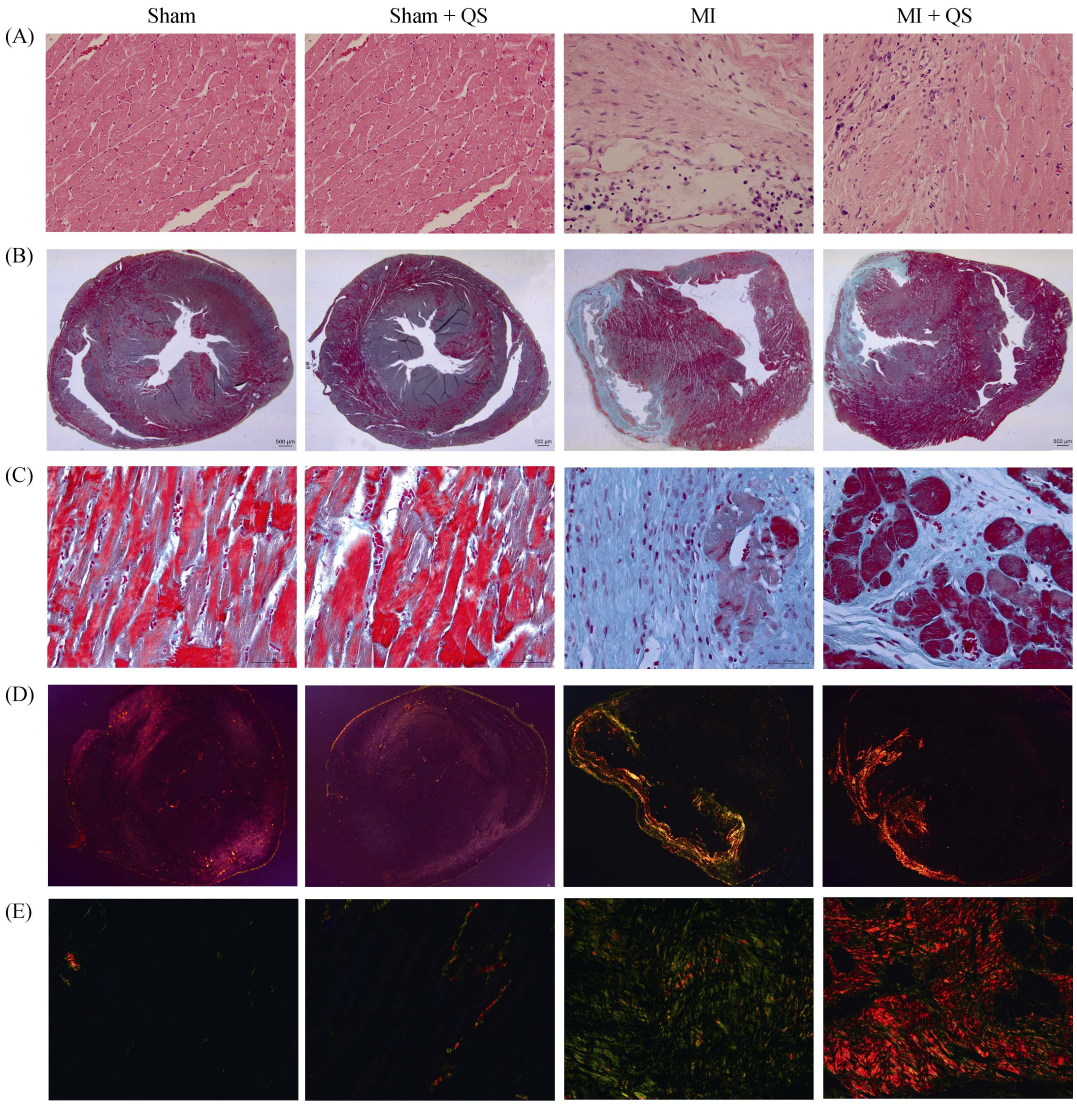

Figure 3. Histopathological staining. (A): Inflammatory cell infiltration shown with Hematoxylin-eosin staining; (B): fibrosis shown with Masson's trichrome staining (12.5 ×); (C): fibrosis shown with Masson's trichrome staining (400 ×); (D): picrosirius red staining to detect the collagen content within the infarct zone (12.5 ×); and (E): picrosirius red staining to detect the collagen content within the infarct zone (400 ×). $n = 3$ in each group. MI: myocardial infarction; QS: Qishen capsule.

was observed after QS treatment (Figure 3B & 3C). Consistent with Masson's trichrome staining, picrosirius red staining also manifested collagen deposition after MI. Moreover, in contrast with the MI group, collagen type I was more prevalent than collagen type III in the QS-treated group, suggesting reduction in collagen content after QS treatment (Figure 3D & 3E).

3.3.3 Myocardial viability in the peri-infarct region

To examine myocardial viability in the peri-infarct region, we immunohistochemically detected the expression of desmin and α-actinin in this region. Concomitant with Masson's trichrome staining, expression of desmin and α-actinin occurred in a larger area in the MI + QS group compared with the MI group, suggesting enhanced myocardial viability after QS administration (Figure 2E).

3.4 QS protected against ultrastructural damage to the myocardial damage

3.4.1 Cardiomyocyte ultrastructure

TEM examination of myocardial ultrastructure revealed sarcomeric disorganization in the left ventricle. Compared with the MI group, more mitochondria were observed in the MI + QS group, which indicates accumulation of abnormal mitochondria. These results suggest that QS treatment improved mitochondrial respiratory function. Furthermore,

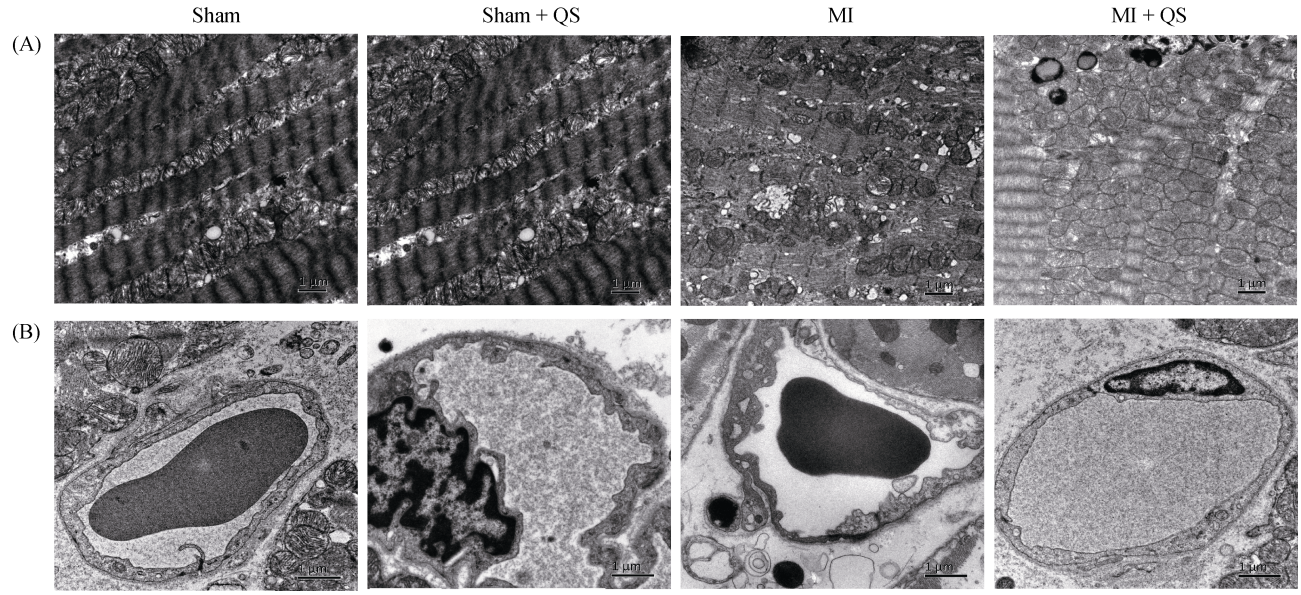

Figure 4. Ultrastructural analysis of the myocardial and capillary architecture. (A): Representative transmission electron microscopy images of the mitochondrial morphology. Mitochondrial swelling with loss of cristae and mitochondria changed to vacuoles were detected in the MI group; and (B): representative transmission electron microscopy images of the capillary architecture, and we found endothelial edema and endoplasmic reticulum expansion in the MI group. MI: myocardial infarction; QS: Qishen capsule.

improved mitochondrial swelling, reduced loss of cristae, and decreased numbers of mitochondria and vacuoles were observed in QS-treated cardiomyocytes (Figure 4A).

3.4.2 Capillary ultrastructure

The ultrastructural morphology of endothelial cells were examined using 12000 × images of capillaries, to determine whether capillary structure was altered. Interestingly, endoplasmic reticulum expansion, swelling, and cytoplasmic vacuoles were detected in the MI group; however, QS-treated rats exhibited normal ultrastructure similar to the sham group (Figure 4B). These findings demonstrate the ultrastructural benefits of QS therapy to capillaries.

3.5 QS therapy induced angiogenesis in both peri-infarct and infarct zones

Use of immunohistochemistry to evaluate capillary density post-MI revealed that QS treatment tripled the number of CD31-positive capillaries in the infarct zone and peri-infarct area compared with the MI group ($P < 0.05$, Figure 5D-F). Moreover, arteriole density (calculated as vessels positive for α-SMA) and was upregulated two-fold in the MI + QS group compared with the MI group ($P < 0.05$, Figure 5B & 5C).

Both the protein and mRNA expression were examined to determine whether the regenerative growth factor VEGF led to increased vascular density. Upon detecting VEGF protein in sham and MI groups, we found that MI caused a significant increase in VEGF levels ($P < 0.05$, Figure 6A). Moreover, compared with MI animals, QS therapy significantly increased VEGF protein levels ($P < 0.05$). This result was confirmed by a marked increase in the intensity of immunofluorescent VEGF staining in the MI + QS group compared with the MI group (Figure 5A). Furthermore, mRNA expression of both VEGF and HIF-1α was detected by qPCR. The results reflected augmented expression of both markers in the MI + QS group compared with the MI group (Figure 6B). We also found that QS treatment enhanced HIF-1α mRNA levels. Collectively, these changes may reflect, at least partially, the cardioprotective effects elicited by QS in angiogenesis.

3.6 QS treatment induced changes in protective signaling

To further explore the mechanism underlying protective roles of QS, expression and activities of protein kinase B (Akt) and MEK/ERK were detected by western blot. As shown in Figure 7, Akt phosphorylation was markedly attenuated, while MEK and ERK phosphorylation were upregulated in the MI group compared with the sham group. Akt phosphorylation was increased, and MEK and ERK phosphorylation were significantly decreased in the MI + QS group compared with the MI group ($P < 0.05$).

4 Discussion

In the present study, we employed QS in a Sprague-Dawley rat model of MI to demonstrate that QS therapy

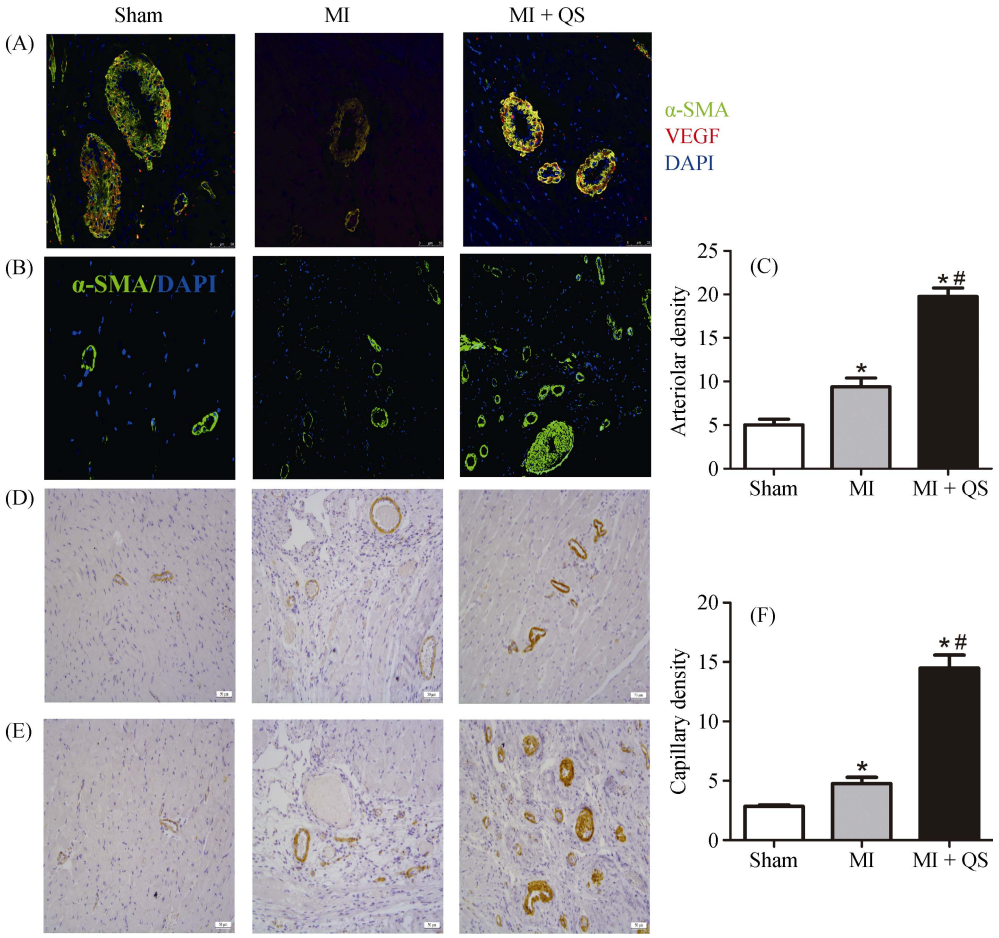

Figure 5. Immunohistochemistry and immunofluorescence assessment of myocardial angiogenesis. (A): Immunofluorescence for the expression of angiogenesis positive for VEGF and α-SMA in the vascular endothelium; (B): sections were stained with α-SMA staining for the arteriolar density measurement; (C): quantification of the arteriolar density; (D): CD31 immunostaining to identify capillaries in the peri-infarct region; (E): CD31 immunostaining to identify capillaries in the infarct region; and (F): quantification of the capillary density. n = 6 in per group. The magnification for A is 400 ×, for B, D and E is 200 ×. $^{*}P < 0.05$ compared with the Sham group, $^{\#}P < 0.05$ compared with the MI group. MI: myocardial infarction; QS: Qishen capsule.

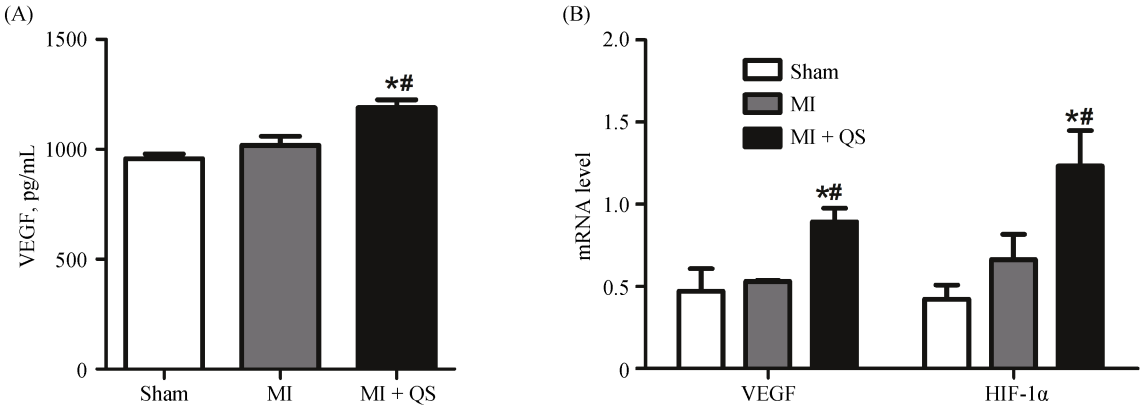

Figure 6. QS treatment increased the levels of VEGF and HIF-1α. (A): The protein level of VEGF from enzyme-linked immunosorbent assay; and (B): the mRNA levels of VEGF and HIF-1α from quantitative real-time polymerase chain reaction. $^{*}P < 0.05$ compared with the Sham group, $^{\#}P < 0.05$ compared with the MI group. HIF-1α: hypoxia inducible factor-1α; MI: myocardial infarction; QS: Qishen capsule; VEGF: vascular endothelial growth factor.

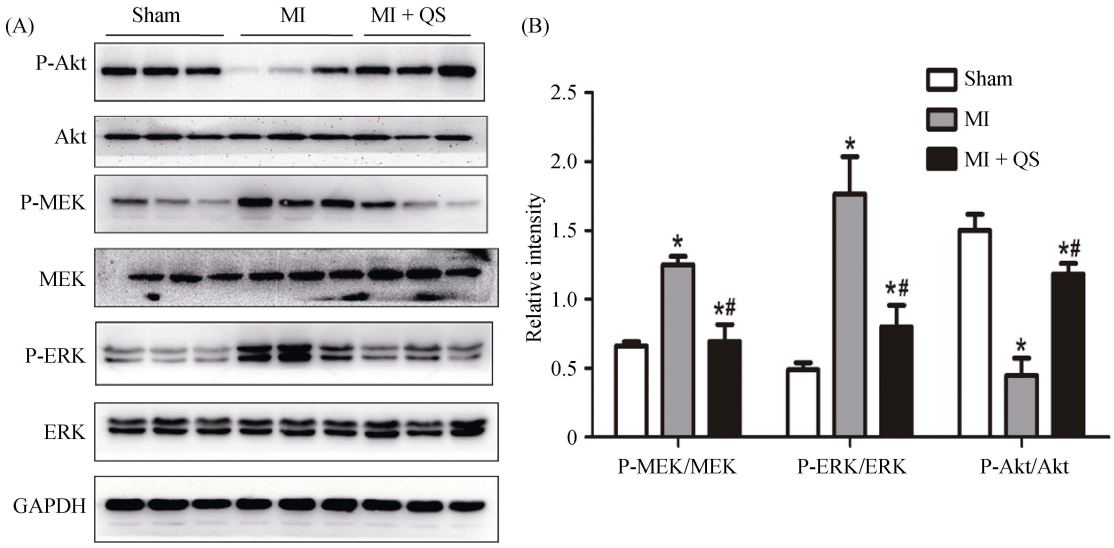

Figure 7. The activities of the Akt and MEK/ERK1/2 pathways were detected with western blotting. (A): The phosphorylation of MEK and ERK1/2 was attenuated markedly by QS in the post-infarct hearts, whereas the phosphorylation of Akt increased; and (B): the histogram shows the relative protein levels of the phosphorylation of Akt and MEK/ERK1/2. The data represent the results of three separate experiments. The results are expressed as the means ± SD. $^{*}P < 0.05$ compared with the Sham group, $^{\#}P < 0.05$ compared with the MI group. Akt: protein kinase B; ERK: extracellular regulated protein kinase; GAPDH: glyceraldehyde-3-phosphate dehydrogenase; MEK: mitogen-activated protein kinase; MI: myocardial infarction; QS: Qishen capsule.

improved cardiac function and attenuated LV remodeling after MI. After four weeks of QS treatment, the MI + QS group exhibited improved cardiac function, reduced infarct scar size and area, increased thinning ratio, as well as attenuation of cardiac weight index and interstitial fibrosis. More interestingly, QS treatment enhanced angiogenesis after chronic ischemic insult.

After MI, progressive occlusion of capillaries and arteries often leads to the development of collateral vessels that supply the ischemic tissue.[19]

However, angiogenesis is normally unable to compensate for the decreased blood supply, leading to the death of otherwise viable myocardium and fibrous substitution.[20] Thus, endogenous myocardial neovascularization is an important pathway enabling cardiac functional recovery after MI.[21,22] In the present study, we observed increased angiogenesis in QS-administered rats, which may be a crucial contributor to the improvement in cardioprotective efficacy. VEGF, the most widely studied agent in trials, has been shown to induce functionally significant angiogenesis in numerous preclinical studies of angiogenic therapies for ischemic heart disease.[23] Our data suggest that QS therapy increased VEGF expression at both protein and mRNA levels. Additionally, we found that 4-week treatment with QS promoted HIF-1α expression. Results from previous studies indicated that HIF-1α transcription can induce expression of many angiogenesis-related genes, including VEGF and its receptors.[24] Therefore, we predicted that QS treatment after MI may enhance VEGF expression via an increased HIF-1α expression, thereby protecting endothelial cells, accelerating endothelial progenitor cell recruitment, and boosting vascular development to promote angiogenesis.

The Akt pathway plays a vital role in inducing cardiac angiogenesis and inhibiting cardiomyocyte apoptosis after MI.[25,26] We identified a pronounced myocardial inhibition of Akt after MI, indicating that the many favorable physiological activities mediated by the Akt pathway are impaired by cardiac dysfunction. However, rats administered by QS exhibited augmented activities of physiological Akt. Early studies demonstrated that phosphorylation of the serine/threonine protein kinase Akt can promote angiogenic behavior.[27,28] Moreover, as demonstrated by many studies, activation of the Akt pathway elicits increased translation of HIF-1α and VEGF mRNA, which leads to angiogenesis.[29] In addition, we found that QS could impact expression levels of Bcl2 and Bax, two downstream proteins associated with the Akt pathway in apoptosis, suggesting that the anti-apoptotic effects of QS were at least partially related to activation of Akt signaling. Thus, QS treatment promoted cardioprotective efficacy in rats after MI though effects related to increased angiogenesis, partially via activation of physiological Akt.

Interestingly, but consistent with a recent study,[15] we also found that post-infarcted rat hearts activated phos-

phorylation of MEK and downstream ERK, whereas QS treatment significantly inhibited this effect. Modulation of the MEK/ERK pathway (for example, by therapeutic strategies involving insulin-like growth factor, statins, or ischemic postconditioning) is a universally recognized and classical mechanism for the treatment of myocardial ischemia injury.[30] However, the effects of QS on MEK/ERK remain uncertain. On the one hand, these results suggest that MEK/ERK inhibition, rather than activation, may contribute to the cardioprotective effects of QS. On the other hand, consistent with a recent study, elevated expression of Akt can result in suppression of the MEK/ERK pathway.[31] Thus, further studies are required to identify the exact cardioprotective mechanisms of MEK/ERK inhibitors.

QS is a TCM comprising extractions or powders from various natural herbs. Based on the results of high-performance liquid chromatography, ginsenoside Rg1 is a basic component of QS. Importantly, ginsenoside Rg1 was shown to protect against myocardial injury after MI.[32,33] In addition, other major ingredients of QS, such as Astragalus and tanshinone, were demonstrated to have beneficial effects on cardiomyocyte dysfunction; for example, by suppressing cardiomyocyte apoptosis and protecting endothelial cells.[34,35] Notably, recent studies have reported the increased effectiveness of multi-target therapy in combating polygenic diseases compared with monotherapies.[36] These studies may partly elucidate the protective mechanisms of QS against ischemic injury after MI.

4.1 Limitations

We acknowledge that this study has some limitations. Firstly, we calculated the concentration of QS used in this study according to the most suitable concentration for adult humans and ratio of rat-to-human body weight; however, this may not be the optimal dose for rats. Regardless, the current study demonstrated that QS treatment could improve cardiac function and attenuate adverse myocardial remodeling, indicating cardioprotective effects of QS. Secondlty, thousands of years of history have established that compound TCM prescriptions (rather than monotherapies) have better therapeutic efficacy, and changes in compatibility proportions may elicit different clinical results. Thus, further studies are needed to identify the most appropriate compatibility proportion of QS for cardioprotection. Last but not least, although QS treatment was shown to promote cardioprotective effects by inhibiting the MEK/ERK signaling pathway, how such inhibition affects other organs, such as liver and kidney, remains unknown. Therefore, further studies are required to examine the influence of QS on other organs.

4.2 Conclusions

We found that QS therapy can improve cardiac function, reduce infarct scar size and area, increase thinning ratio, as well as attenuation of cardiac weight index and interstitial fibrosis in a Sprague-Dawley rat model of MI. Furthermore, QS treatment enhanced angiogenesis after chronic ischemic insult, at least partially via activation of the Akt signaling pathway and inhibition of MEK/ERK phosphorylation.

Acknowledgments

This study was supported by the Fuwai Hospital (No. 2013-ZX009). The authors thank Doctor Li WANG and Sheng-Hua LIU for the contributions in experimental design and performed experiments. All authors had no conflicts of interest to disclose.

References

1 Cavasin MA, Tao Z, Menon S, *et al*. Gender differences in cardiac function during early remodeling after acute myocardial infarction in mice. *Life Sci* 2004; 75: 2181–2192.

2 Van den Borne SW, Cleutjens JP, Hanemaaijer R, *et al*. Increased matrix metalloproteinase-8 and -9 activity in patients with infarct rupture after myocardial infarction. *Cardiovasc Pathol* 2009; 18: 37–43.

3 Ortiz-Pérez JT, Riera M, Bosch X, *et al*. Role of circulating angiotensin converting enzyme 2 in left ventricular remodeling following myocardial infarction: a prospective controlled study. *PLOS One* 2013; 8: e61695.

4 Albrecht-Schgoer K, Schgoer W, *et al*. The angiogenic factor secretoneurin induces coronary angiogenesis in a model of myocardial infarction by stimulation of vascular endothelial growth factor signaling in endothelial cells. *Circulation* 2012; 126: 2491–2501.

5 Zhou Q, Gallagher R, Ufret-Vincenty R, *et al*. Regulation of angiogenesis and choroidal neovascularization by members of microRNA-23~27~24 clusters. *Proc Natl Acad Sci U S A* 2011; 108: 8287–8292.

6 Lassaletta AD, Chu LM, Sellke FW. Therapeutic neovascularization for coronary disease: current state and future prospects. *Basic Res Cardiol* 2011; 106: 897–909.

7 Wang ZT, Zhang SJ, Han LH, *et al*. Effects of xuesetong soft capsules on angiogenesis and VEGF mRNA expression in ischemic myocardium in rats with myocardial infarction. *J Tradit Chin Med* 2012; 32: 71–74.

8 Liu X, Jiang Y, Yu X, *et al*. Ginsenoside-Rb3 protects the myocardium from ischemia-reperfusion injury via the inhibition of apoptosis in rats. *Exp Ther Med* 2014; 8: 1751–1756.

9 Bai WW, Xing YF, Wang B, *et al*. Tongxinluo improves cardiac function and ameliorates ventricular remodeling in mice model of myocardial infarction through enhancing

angiogenesis. *Evid Based Complement Alternat Med* 2013; 2013: 813247.
10 Yuan QL, Gao GM. Influences of Qishen capsules on hemorheology and heart function in patients with coronary heart disease. *Zhong Guo Shi Yong Yi Yao* 2013; 8: 142–143. [In Chinese].
11 Wu YB, Li YM, Tang H, *et al*. The clinical application of Qishen capsule in patients with cardiac arrhythmia after acute myocardial infarction. *Zhong Guo Zhong Yi Ji Zheng* 2012; 21: 1314–1315. [In Chinese].
12 Campbell DJ, Somaratne JB, Jenkins AJ, *et al*. Differences in myocardial structure and coronary microvasculature between men and women with coronary artery disease. *Hypertension* 2011; 57: 186–192.
13 Campbell DJ, Somaratne JB, Jenkins AJ, *et al*. Reduced microvascular density in non-ischemic myocardium of patients with recent non-ST-segment-elevation myocardial infarction. *Int J Cardiol* 2013; 167: 1027–1037.
14 Zhang YL, Yao YT, Fang NX, *et al*. Restoration of autophagic flux in myocardial tissues is required for cardioprotection of sevoflurane postconditioning in rats. *Acta Pharmacol Sin* 2014; 35: 758–769.
15 Zhang Q, Wang H, Yang YJ, *et al*. Atorvastatin treatment improves the effects of mesenchymal stem cell transplantation on acute myocardial infarction: the role of the RhoA/ROCK/ERK pathway. *Int J Cardiol* 2014; 176: 670–679.
16 Zhao ZQ, Puskas JD, Xu D, *et al*. Improvement in cardiac function with small intestine extracellular matrix is associated with recruitment of C-kit cells, myofibroblasts, and macrophages after myocardial infarction. *J Am Coll Cardiol* 2010; 55: 1250–1261.
17 Kitahara T, Takeishi Y, Harada M, *et al*. High-mobility group box 1 restores cardiac function after myocardial infarction in transgenic mice. *Cardiovasc Res* 2008; 80: 40–46.
18 Ilhan A, Gartner W, Neziri D, *et al*. Angiogenic factors in plasma of brain tumour patients. *Anticancer Res* 2009; 29: 731–736.
19 Khan TA, Sellke FW, Laham RJ. Gene therapy progress and prospects: therapeutic angiogenesis for limb and myocardial ischemia. *Gene Ther* 2003; 10: 285–291.
20 Ding L, Dong L, Chen X, *et al*. Increased expression of integrin-linked kinase attenuates left ventricular remodeling and improves cardiac function after myocardial infarction. *Circulation* 2009; 120: 764–773.
21 Kalkman EA, Bilgin YM, van Haren P, *et al*. Determinants of coronary reserve in rats subjected to coronary artery ligation or aortic banding. *Cardiovasc Res* 1996; 32: 1088–1095.
22 Nelissen-Vrancken HJ, Debets JJ, Snoeckx LH, *et al*. Time-related normalization of maximal coronary flow in isolated perfused hearts of rats with myocardial infarction. *Circulation* 1996; 93: 349–355.
23 Sim EK, Zhang L, Shim WS, *et al*. Therapeutic angiogenesis for coronary artery disease. *J Card Surg* 2002; 17: 350–354.
24 Trentin D, Hall H, Wechsler S, *et al*. Peptide-matrix-mediated gene transfer of an oxygen-insensitive hypoxia-inducible factor-1alpha variant for local induction of angiogenesis. *Proc Natl Acad Sci U S A* 2006; 103: 2506–2511.
25 Patten RD, Pourati I, Aronovitz MJ, *et al*. 17beta-estradiol reduces cardiomyocyte apoptosis in vivo and in vitro via activation of phospho-inositide-3 kinase/Akt signaling. *Circ Res* 2004; 95: 692–699.
26 He Z, Opland DM, Way KJ, *et al*. Regulation of vascular endothelial growth factor expression and vascularization in the myocardium by insulin receptor and PI3K/Akt pathways in insulin resistance and ischemia. *Arterioscler Thromb Vasc Biol* 2006; 26: 787–793.
27 Zachary I, Gliki G. Signaling transduction mechanisms mediating biological actions of the vascular endothelial growth factor family. *Cardiovasc Res* 2001; 49: 568–581.
28 Olsson AK, Dimberg A, Kreuger J, *et al*. VEGF receptor signalling-in control of vascular function. *Nat Rev Mol Cell Biol* 2006; 7: 359–371.
29 Bárdos JI, Ashcroft M. Negative and positive regulation of HIF-1: a complex network. *Biochim Biophys Acta* 2005; 1755: 107–120.
30 Hausenloy DJ, Yellon DM. Reperfusion injury salvage kinase signalling: taking a RISK for cardioprotection. *Heart Fail Rev* 2007; 12: 217–234.
31 Ahn YT, Shin IJ, Kim JM, *et al*. Counteracting the activation of pAkt by inhibition of MEK/Erk inhibition reduces actin disruption-mediated apoptosis in PTEN-null PC3M prostate cancer cell lines. *Oncol Lett* 2013; 6: 1383–1389.
32 Zhou H, Hou SZ, Luo P, *et al*. Ginseng protects rodent hearts from acute myocardial ischemia-reperfusion injury through GR/ER-activated RISK pathway in an endothelial NOS-dependent mechanism. *J Ethnopharmacol* 2011; 135: 287–298.
33 Zhu D, Wu L, Li CR, *et al*. Ginsenoside Rg1 protects rat cardiomyocyte from hypoxia/reoxygenation oxidative injury via antioxidant and intracellular calcium homeostasis. *J Cell Biochem* 2009; 108: 117–124.
34 Li X, Qu L, Dong Y, *et al*. A review of recent research progress on the astragalus genus. *Molecules* 2014; 19: 18850–18880.
35 Sun D, Shen M, Li J, *et al*. Cardioprotective effects of tanshinone IIA pretreatment via kinin B2 receptor-Akt-GSK-3beta dependent pathway in experimental diabetic cardiomyopathy. *Cardiovasc Diabetol* 2011; 10: 4.
36 Li X, Wu L, Liu W, *et al*. A network pharmacology study of Chinese medicine QiShenYiQi to reveal its underlying multi-compound, multi-target, multi-pathway mode of action. *PLoS One* 2014; 9: e95004.